RSC Advances

ROYAL SOCIETY OF CHEMISTRY

www.rsc.org/advances

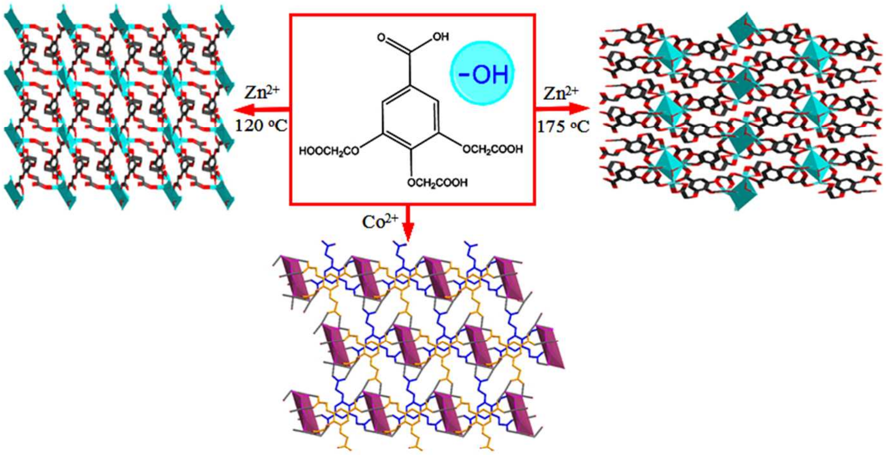

254x190mm (96 x 96 DPI)

Cite this: DOI: 10.1039/c0xx00000x

www.rsc.org/advances

PAPER

Self-assembly, crystal structures and properties of metal-3,4,5-tris (carboxymethoxy)benzoic acid frameworks based on polynuclear metal-hydroxyl clusters (M = Zn, Co)

Gaoshan Yang,[a] Huiliang Wen,[b] Chongbo Liu,[*ac] Julianne Robbins,[c] Yunhan Wen[d] and Z. John Zhang[*c]

Received (in XXX, XXX) Xth XXXXXXXXX 20XX, Accepted Xth XXXXXXXXX 20XX
DOI: 10.1039/b000000x

3,4,5-Tris(carboxymethoxy)benzoic acid (H_4TCBA) has been used as structure-directing agent to prepare three new inorganic−organic hybrid frameworks based on polynuclear metal-hydroxyl clusters, $[Zn_{2.5}(OH)(TCBA)(H_2O)_4]\cdot H_2O$ (**1**), $[Zn_{2.5}(OH)(TCBA)(H_2O)]$ (**2**), $[Co_3(OH)_2(TCBA)(H_2O)_4]\cdot 2H_2O$ (**3**) through hydro/solvothermal reactions. The results show that complexes **1** and **2** both own I^0O^3 hybrid frameworks with a highly-connected binodal 4,8-c network, while **3** reveals I^0O^2 hybrid framework with a 3,6-c 2-nodal topology. The multiple coordination system originated from the branching out carboxylate groups in TCBA ligands results in the formation of the multi-stranded helical chains in the high-dimensional metal-organic frameworks of complexes **1**−**3**. The thermal stabilities of complexes **1**−**3**, the photophysical properties of complexes **1** and **2** and the magnetic properties of complex **3** were also investigated. Complexes **1** and **2** emit strong blue light at ultraviolet light, and complex **3** shows typical paramagnetic behavior and an interesting partial spin-crossover has been observed.

Introduction

Recently, much attention has been paid to the design and synthesis of novel metal-organic frameworks (MOFs) based on multinuclear metal clusters not only for the diversity of their structures and topologies, but also for their potential applications in various fields such as gas storage/separation,[1] catalysis,[2] photoluminescence[3] and magnetics.[4] Polynuclear hydroxyl-containing SBUs are a good selection for the formation of stable MOFs.[5]

In recent years complicated MOFs with multinuclear metal clusters have usually been interpreted using a network topological approach. This approach reduces complicated polynuclear clusters to simple node-and-linker nets for the analysis, comparison, and design of MOFs materials.[6] Up to now, the frameworks containing a single metal centre with a connection over eight are rarely observed. Numerous studies show that the use of multinuclear metal clusters as nodes is probably an effective route to generate higher connected topology nets owing to the increased coordination numbers and reduced steric hindrance of metal clusters.[7] The involvement of hydroxyl ligands should increase the topological connectivity in the frameworks.

On the other hand, tremendous advancements in the field of hybrid inorganic-organic framework materials has achieved over the past decade. In these single phased hybrid materials, inorganic components can provide various physical and chemical functionalities through the structures and metal species. The organic components can greatly expand the structural diversities and build flexibilities into the structures through judiciously chosen organic molecules. According to the classification made by Cheetham, Rao and Feller, the vast number of hybrid inorganic-organic frameworks cotain two parts: metal–organic and metal-inorganic networks.[8] The dimensionality of organic frameworks was defined with ‘metal to organic ligand to metal’ (M−L−M) connectivity and the dimensionality of inorganic frameworks by M−X−M (X = O, N, Cl, S) connectivity. Therefore, the structural dimensionality of a hybrid framework can be represented with a simple notion of I^nO^m, where I^n ($n = 0−3$) is the dimensionality of inorganic structure (M−X−M) and O^m ($m = 0−3$) as organic ligand-based dimensionality (M−L−M).

The design of helical coordination polymers has attracted a lot of attention recently because of the frequent appearance of helix structures in proteins, collagens, quartz and single-walled carbon nanotubes.[9] Commonly, much effort has been devoted to the preparation of helical coordination polymers with metals in the backbone by using specifically designed bridging ligands such as flexible and angular ditopic ligands, rigid and hinge-like ditopic ligands, and some rigid pyridine- or carboxylate-based ligands.[10] For instance, multicarboxylate ligands have been used to construct helical coordination polymers. These kinds of ligands are usually employed as flexible carboxylate ligands such as succinic and glutaric acids,[11] or as rigid carboxylate ligands such as benzenedicarboxylate, benzenetricarboxylate for building up helix structures within the frameworks.[11b,12] We considered the polycarboxylate ligand, 3,4,5-tris(carboxymethoxy)benzoic acid as a good candidate for the above purpose. H_4TCBA ligand possesses one rigid carboxyl group and three flexible oxyacetate groups. The four carboxyl groups branch out in three different angles of 60°, 120°, 180°, which should help to link metal ions in a plurality of directions to facilitate the formation of multi-stranded helices, together with hydroxyl groups, further to construct hybrid inorganic-organic frameworks with polynuclear clusters and high connectivity. Herein we report the syntheses of three new hybrid inorganic-organic frameworks based on H_4TCBA and hydroxyl groups, $[Zn_{2.5}(OH)(TCBA)(H_2O)_4]\cdot H_2O$ (**1**), $[Zn_{2.5}(OH)(TCBA)(H_2O)]$ (**2**), $[Co_3(OH)_2(TCBA)(H_2O)_4]\cdot 2H_2O$ (**3**). These complexes all show interesting structural frameworks and topology with intertwined helical structures. Complexes **1** and **2** emit strong blue light at ultraviolet light, and complex **3** shows typical paramagnetic behavior and an interesting partial spin-crossover has been observed.

Experimental

Ligands. 3,4,5-tris(carboxymethoxy)benzoic acid was prepared according to the literature methods.[13] The details can be found in supplementary documents. All chemical reagents were obtained from commercial sources and used as received. Elemental analyses were performed with an Elementar Vario EL analyzer and IR spectra were measured as KBr discs on a Nicolet Avatar 5700 FT-IR spectrometer in the 4000−400 cm^{-1} region. ^{1}H-NMR spectra were recorded at 400 MHz on a Bruker WH400 DS spectrometer. Mass spectra were measured on an Agilent Liquid chromatography-mass analyzer spectrometry (LC-MS) 1100 series instrument in the electrospray ionization [negative electrospray ionization (ESI)] mode. Fluorescence measurements were made on a Hitachi F-7000 fluorophotometer at room temperature. Thermogravimetric curves were recorded with a Perkin-Elmer Diamond TG/DTA Thermal Analyzer, a platinum container was used for heating the sample with a heating rate of 10 °C/min under a N_2 atmosphere. Powder X-ray diffraction (PXRD) measurements were performed on a Bruker D8-DVANCE X-ray diffractometer with Cu Kα radiation (λ = 1.5418 Å). Temperature-dependent magnetization measurements were carried out on a superconducting quantum interference device (SQUID) magnetometer (Quantum Design MPMS-5S).

Synthesis of $[Zn_{2.5}(OH)(TCBA)(H_2O)_4]\cdot H_2O$ (1). A mixture of $ZnCl_2\cdot 4H_2O$ (0.021 g, 0.1 mmol), H_4TCBA (0.034 g, 0.1 mmol), NaOH (0.3 mmol), distilled water (7 mL) and isopropanol (3 mL) was sealed in a Teflon-lined stainless reactor (23 mL) and heated 120 °C for 72 h under autogenous pressure. Colorless block crystals were obtained. Yield: 16.1% (based on Zn). Anal. Calcd. for $C_{13}H_{19}Zn_{2.5}O_{17}$ (%): C 25.56; H 3.14. Found: C 25.72; H 3.26. IR data (KBr pellet, ν/cm^{-1}): 3421 (s), 1607 (vs), 1402 (vs), 1333 (m), 1264 (w), 1217 (w), 1131 (m), 1065 (w), 780 (w), 630 (w).

Synthesis of $[Zn_{2.5}(OH)(TCBA)(H_2O)]$ (2). The synthesis of **2** was similar with that of **1**, except the reaction temperature was raised to 175 °C. Colorless block crystals were obtained. Yield: 20.2% (based on Zn). Anal. Calcd. for $C_{13}H_{11}O_{13}Zn_{2.5}$ (%): C 28.98; H 2.06. Found: C 28.75; H 2.45. IR data (KBr pellet, ν/cm^{-1}): 3440 (s), 3133 (vs), 1608 (s), 1401 (s), 1324 (w), 1204 (w), 1137 (m), 1075 (w), 1038 (w), 872 (w), 777 (m), 684 (w).

Synthesis of $[Co_3(OH)_2(TCBA)(H_2O)_4]\cdot 2H_2O$ (3). A mixture of $CoCl_2\cdot 6H_2O$ (0.024 g, 0.1 mmol), H_4TCBA (0.034 g, 0.1 mmol), NaOH (0.2 mmol), distilled water (7 mL) and ethanol (3 mL) was sealed in a Teflon-lined stainless reactor (23 mL) and heated 90 °C for 72 h under autogenous pressure. Red block crystals were obtained. Yield: 18.6 % (based on Co). Anal. Calcd. for $C_{13}H_{22}Co_3O_{19}$ (%): C 23.69; H 3.36. Found: C 23.46; H 2.92. IR data (KBr pellet, ν/cm^{-1}): 3610 (s), 3157 (vs), 1614 (s), 1500 (w), 1406 (s), 1329 (m), 1213 (w), 1132 (m), 1032 (w), 876 (w), 781 (m), 728 (w), 691 (w).

Single-crystal x-ray measurements. The single-crystal X-ray data of **1**−**3** were collected on a Brucker APEX II area detector diffractometer with a graphite-monochromated Mo Ka radiation (λ = 0.71073 Å). Semi-empirical absorption corrections were applied to the title complexes using the SADABS program.[14] The structures were solved by direct methods,[15] and refined by full-matrix least squares on F^2 using SHELXL-97.[16] All non-hydrogen atoms were refined anisotropically. The hydroxyl H and water H atoms were located from difference Fourier maps, the other hydrogen atoms were placed in geometrically calculated positions. CCDC reference numbers are 999328−999330. These data can be obtained free of charge from The Cambridge Crystallographic Data Center via www.ccdc.cam.ac.uk/data_request/cif. Experimental details for X-ray data collection of **1**−**3** are presented in Table 1, and selected bond lengths are listed in Table S1,† and the selected hydrogen bonding lengths and angles are listed in Table S2.†

Table 1 Crystal data for complexes **1**−**3**

Complex	**1**	**2**	**3**
Empirical formula	$C_{13}H_{19}O_{17}Zn_{2.5}$	$C_{13}H_{11}O_{13}Zn_{2.5}$	$C_{13}H_{22}O_{19}Co_3$
Formula weight	610.71	538.64	659.10
T/K	296(2)	296(2)	296(2)
Crystal system	Triclinic	Monoclinic	Triclinic
Space group	$P\bar{1}$	$P2_1/c$	$P\bar{1}$
a /Å	7.741(1)	8.075(1)	7.947(1)
b /Å	10.007(1)	8.575(1)	12.541(1)
c /Å	12.434(1)	22.703(1)	12.562(1)
α /°	89.732(1)	90	111.680
β /°	89.884(1)	92.166(1)	106.200
γ /°	84.946(1)	90	94.380
V /Å^3	959.4(1)	1570.8(1)	1094.5(1)
Z	2	4	2
F(000)	616	1072	666
D_C/g·cm^{-3}	2.114	2.278	2.000
θ range/°	2.62-25.5	2.52-27.50	2.94-25.49
μ/mm^{-1}	3.203	3.878	2.341
GOF	1.090	1.073	1.066
Reflections collected	7400	13626	8426
Independent reflections	3537	3606	4045
R_{int}	0.0108	0.0188	0.0107
R_1 , wR_2 [$I>2\sigma(I)$]	0.0219, 0.0586	0.0247, 0.0632	0.0277, 0.0737
R_1 , wR_2 (all data)	0.0226, 0.0590	0.0276, 0.0646	0.0303, 0.0755

Results and discussion

Structure of $[Zn_{2.5}(OH)(TCBA)(H_2O)_4]\cdot H_2O$ (1). The asymmetric unit of complex **1** consists of three crystallographically independent Zn(II) cations, one hydroxyl and one TCBA ligand, four coordinated and one lattice water molecules (Fig. 1a). For these three types of Zn(II) cations, each Zn1 lies on an inversion centre and coordinates to six oxygen atoms from two carboxylates, two hydroxyl groups and two water molecules; Zn2 is six coordinated by two water molecules, one hydroxyl and three carboxylate oxygen atoms; while Zn3 is four coordinated by one water molecule, one hydroxyl and two carboxylate oxygen atoms. One TCBA anion bonds to six Zn(II) ions through six carboxylate oxygen atoms, as shown in Fig. 1a.

Hydroxyl oxygen atoms in **1** act in a μ_3-bridging mode connecting one Zn1, one Zn2 and one Zn3 atom (O12 in Fig. 1b). Two hydroxyl oxygen atoms join five Zn atoms forming one centrosymmetric pentameric Zn cluster, as shown in Fig. 1b. 1-carboxylate group, 3- and 4-oxyacetate groups join Zn2 and Zn3 atoms to a double-helical chain with opposite chirality, and the pitch of the helix running along the *b*-axis (20.018 Å) is two times the length of the *b* axis unit (10.009 Å). The chains are further linked through 5-oxyacetate groups and Zn1 atoms, resulting in a 3D M−L−M framework (Fig. 1c). Thus the whole hybrid framework of **1** can be represented with a notion of I^0O^3 (Fig. 1d).

Considering the framework of **1** from a network topological point. One TCBA ligand links six Zn ions from four pentameric units (Fig. 2a), and one $[Zn_5(OH)_2]^{8+}$ cluster joins eight TCBA ligands (Fig. 2b). The topological net of **1** is a 2-nodal (4,8)-connected net with the Schläfli symbol of $\{4^{12}\cdot6^{12}\cdot8^4\}\{4^6\}_2$, in which the ratio of $[Zn_5(OH)_2]^{8+}$ clusters and TCBA anions is 1:2 (Fig. 2c).

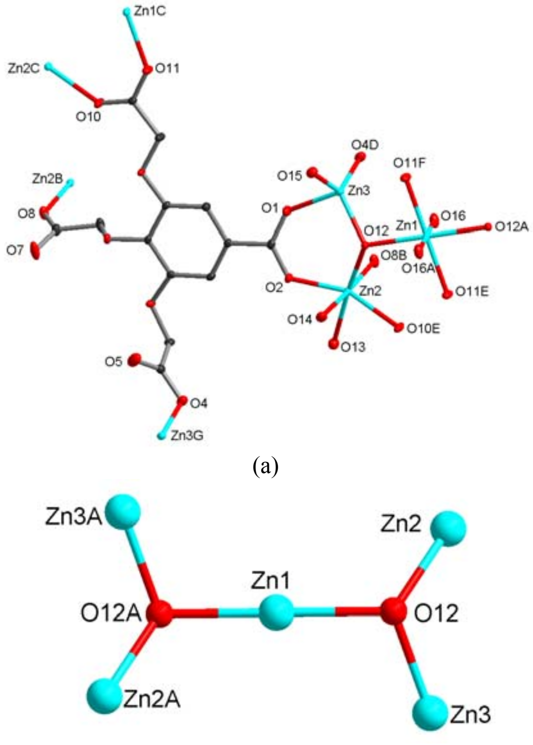

(a)

(b)

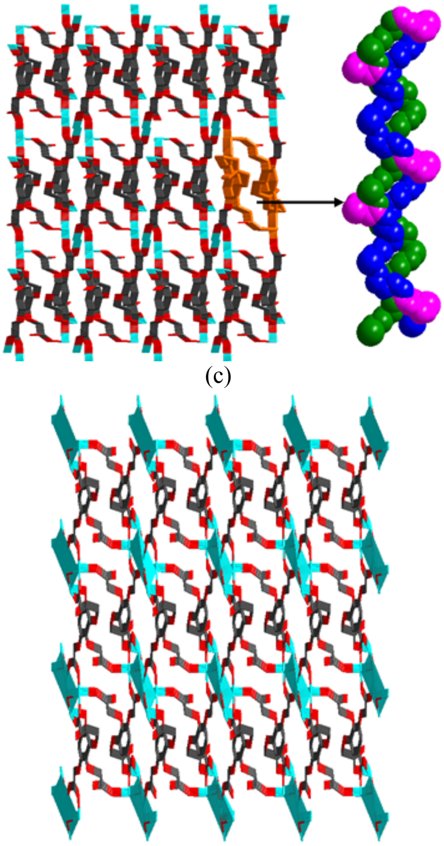

(c)

(d)

Fig. 1 (a) Coordination environment of Zn(II) ion in complex **1**, the asymmetric bridging mode of TCBA and μ_3-OH bridge. (b) $[Zn_5(OH)_2]^{8+}$ cluster. (c) The 3-D organic connectivity with double-stranded helix chains of opposite chirality along *b*-axis after omitting hydroxyl and water molecules; blue: left, green: right, pink: shared atoms. (d) The structure of **1** containing 0-D inorganic (blue) and 3-D organic (gray) connectivity along *b*-axis.

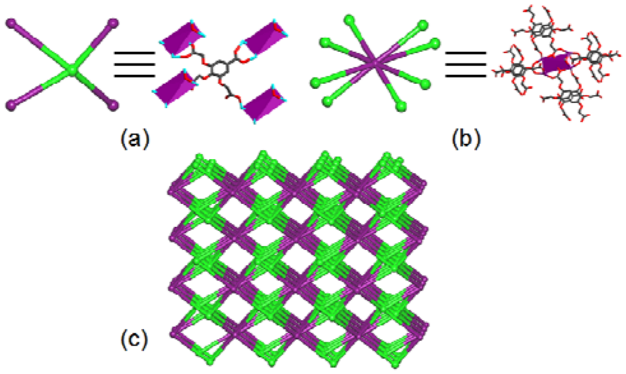

Fig. 2 Schematic representation for the nodes of TCBA anions (a) and $[Zn_5(OH)_2]^{8+}$ cluster (b). (c) The (4,8)-connected topological net in complex **2** (bright green and violet represent TCBA ligands and $[Zn_5(OH)_2]^{8+}$ clusters respectively).

Structure of $[Zn_{2.5}(OH)(TCBA)(H_2O)]$ (2). Compared to **1**, there are also three crystallographically independent Zn(II) ions, one hydroxyl and one TCBA ligand, but only one coordinated water molecule in the asymmetric unit of complex **2** (Fig. 3a). Hydroxyl and TCBA ligands also join three crystallographically independent Zn(II) ions of **2** to an I^0O^3 hybrid framework (Fig.

3d). Zn1 lies on an inversion centre and coordinates to six oxygen atoms: two carboxylate and two hydroxyl oxygen atoms, two water oxygen atoms, which is the same to Zn1 ion in **1**. Zn2 is six coordinated by one hydroxyl, three and two ether oxygen atoms. Zn3 is four coordinated by one hydroxyl and three carboxylate oxygen atoms. However, the coordination environments of Zn2 and Zn3 are different from those of **2** respectively; one TCBA anion bonds to six Zn(II) ions through six carboxylate oxygen and two ether oxygen atoms (Fig. 3a).

The bonding of hydroxyl groups of **2** is similar to that of **1**. Each hydroxyl oxygen atom in **2** links three Zn atoms (Zn1, Zn2 and Zn3), showing a μ_3-bridging mode, two hydroxyl oxygen atoms join five Zn atoms forming one centrosymmetric pentameric Zn cluster (Fig. 3b).

The striking feature of **2** is TCBA ligands join Zn^{2+} ions to form a 3D framework containing double left-helical chains and double right-helical chains (Fig. 3c). The repeating unit of helical chain can be described as $(-Zn2-O5-C9-O4-Zn3-O11-C13-C12-O9-C6-C7-C2-C1-O1-Zn2-O7-Zn1-O7-)_n$. The pitch of the helical running along the *a*-axis (16.15 Å) is two times the length of the *a* axis (8.07 Å). These two double helical chains with opposite chirality are united at Zn1 and O7 atoms. Thus the hybrid framework of complex **2** can also be described as I^0O^3 (Fig. 3d).

From a topological view, one TCBA ligand links six Zn ions from four separate pentameric units (Fig. 4a), and one $[Zn_5(OH)_2]^{8+}$ cluster joins eight TCBA ligands (Fig. 4b). The topological net of **2** is a 2-nodal (4,8)-connected net with the Schläfli symbol of $\{4^{16}\cdot6^{12}\}\{4^4\cdot6^2\}_2$, which is a little different from **1**, in which the ratio of $[Zn_5(OH)_2]^{8+}$ clusters and TCBA anions is also 1:2 (Fig. 4c).

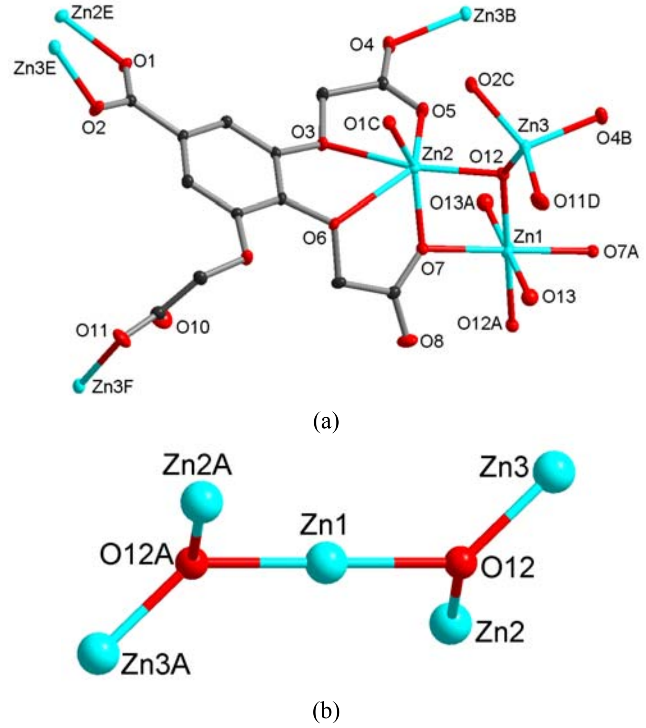

(a)

(b)

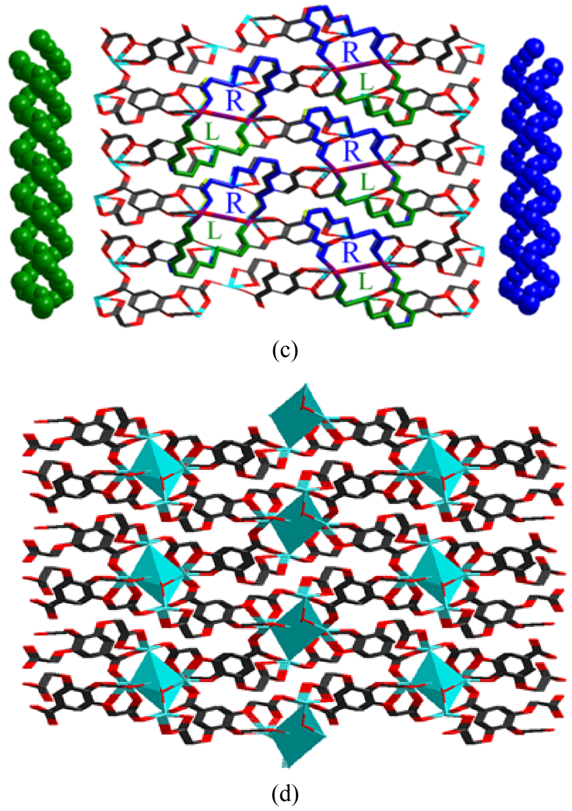

(c)

(d)

Fig. 3 (a) Coordination environment of Zn(II) ion in complex **2**, the asymmetric bridging mode of TCBA and μ_3-OH bridge. (b) $[Zn_5(OH)_2]^{8+}$ cluster. (c) A 3-D organic connectivity with double left-helical chains and double right-helical chains along *a*-axis after omitting hydroxyl and water molecules; blue: right, green: left. (d) The structure of **2** containing 0-D inorganic (blue) and 3-D organic (gray) connectivity along *a*-axis.

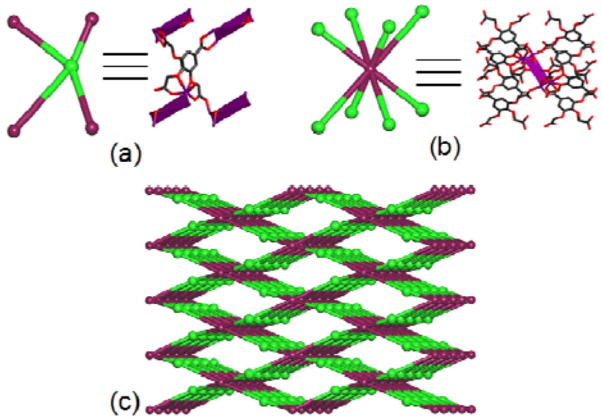

Fig. 4 (a) 4-Connected ligand node. (b) 8-Connected $[Zn_5(OH)_2]^{8+}$ cluster in complex **2**. (c) (4,8)-Connected $(4^{16}\cdot6^{12})(4^4\cdot6^2)_2$ topological net of **2** (bright green and violet represent TCBA ligands and $[Zn_5(OH)_2]^{8+}$ clusters respectively).

Structure of $[Co_3(OH)_2(TCBA)(H_2O)_4]\cdot2H_2O$ (3). The structure of complex **3** contains three crystallographically independent Co(II) ions (Fig. 5a). Co1, Co2 and Co3 ions all are six coordinated, all displaying a distorted octahedral geometry. Six oxygen atoms coordinated to Co1 come from three carboxylate oxygen atoms in three O-acetate groups of three TCBA ligands, two hydroxyl groups and one water molecule.

And those coordinated to Co2 are from one hydroxyl group, two water molecules, and one carboxylate and two O-acetate groups in three TCBA ligands. Those coordinated to Co3 are from three hydroxyl groups, one water molecule and one carboxylate and one O-acetate group in two TCBA ligands. Each hydroxyl oxygen atom links three Co^{2+} cations, exhibits two kinds of μ_3-OH bridging modes. One type of μ_3-OH connects to one Co1, one Co2 and one Co3, and another type bridges to one Co1 and two Co3 atoms. Two sets of these μ_3-OH bridging modes connect together two sets of Co1, Co2 and Co3 cations to form a centrosymmetric hexameric $[Co_6(OH)_4]^{8+}$ cluster (Fig. 5b).

The $[Co_6(OH)_4]^{8+}$ clusters are connected through TCBA ligands to build up a hybrid framework of I^0O^2 type (Fig. 5c). Each TCBA ligand in **3** bonds to eight Co(II) ions through eight carboxylate oxygen atoms to form a bi-layer structure as shown in Fig. 5c, and the phenyl rings of TCBA ligands are distributed in two paralleled planes with the distance of 3.9586 Å. One kind of double helical chains with opposite chirality can be observed in the M−L−M bi-layer, and the repeating unit of helical chain can be described as (−Co2−O1−C1−C2−C7−C6−O9−C12−C13−O11−Co1−O8−C11−C10−O6−C5−C6−O9−C12−C13−O11−Co1−O4−C9−C8−O3−C4−C5−O6−C10−C11−O8−Co2−)$_n$ as shown in Fig. 5d. These 2-D bi-layers stuck into a 3-D supramolecular structure (Fig. 5d) through rich hydrogen bonds (as shown in Table S2.†).

Apparently, the octahedral $[Co_6(OH)_4]^{8+}$ cluster and TCBA ligand in **3** can be viewed as two subunits. Therefore, each TCBA ligand linking three $[Co_6(OH)_4]^{8+}$ clusters can be regarded as a 3-connected node (Fig. 6a). Each $[Co_6(OH)_4]^{8+}$ unit, surrounded by six TCBA ligands, can be considered as an 6-connected node (Fig. 6b), and the ratio of $[Co_6(OH)_4]^{8+}$ and TCBA anions is 1:2. Consequently, the topological net of **3** is (3,6)-connected net with the Schläfli symbol of $\{4^3\}_2\{4^6{\cdot}6^6{\cdot}8^3\}$ (Fig. 6c).

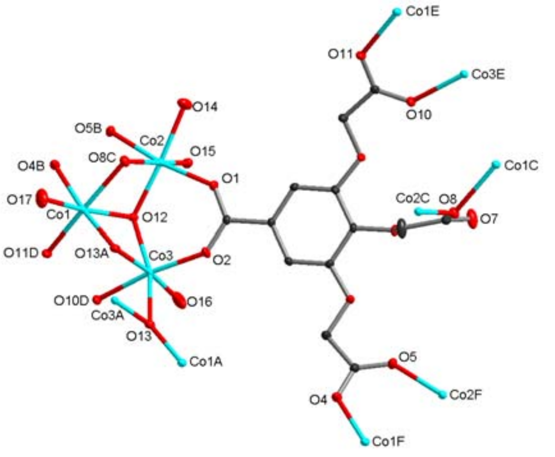

(a)

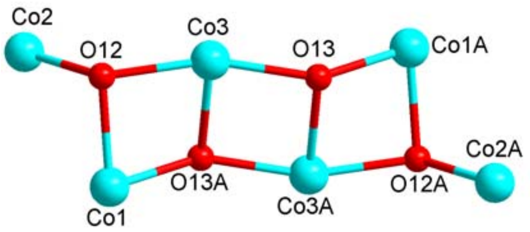

(b)

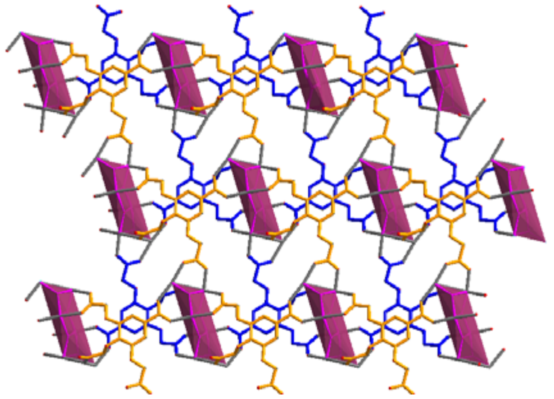

(c)

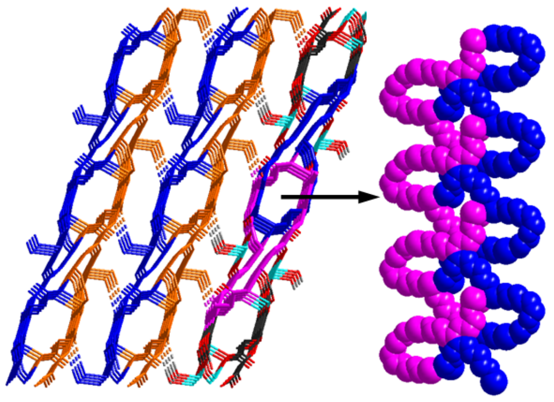

(d)

Fig. 5 (a) Coordination environment of Co(II) ion in complex **3**, the asymmetric bridging mode of TCBA and μ_3-OH bridge. (b) $[Co_6(OH)_4]^{8+}$ cluster. (c) The I^0O^2 hybrid framework of **3** containing 0-D inorganic and 2-D organic connectivity along *a*-axis. (d) 3-D supramolecular structure with double helical chains of opposite chirality along *b*-axis after ommitting μ_3-OH groups; pink: right, blue: left.

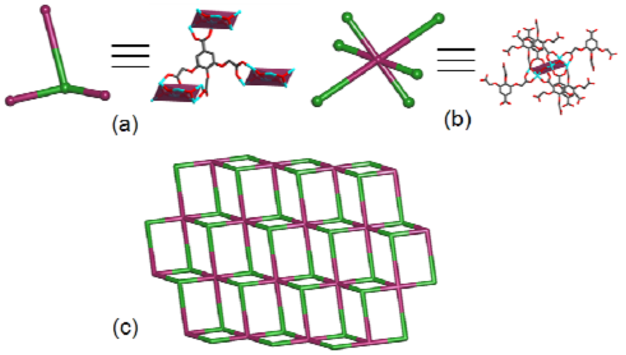

Fig. 6 (a) 3-Connected ligand node. (b) 6-Connected $[Co_6(OH)_2]^{8+}$ cluster in complex **3**. (c) (3,6)-Connected $\{4^3\}_2\{4^6{\cdot}6^6{\cdot}8^3\}$ topological net of **3** (green and plum represent TCBA ligands and $[Co_6(OH)_4]^{8+}$ clusters respectively).

Effect of the metal ions and temperature on structural diversity. Complexes **1** and **2** exhibit a highly-connected binodal (4,8-c) net with different topology, and complex **3** shows a 3,6-c 2-nodal topology, so the results from the structural analyses of these three hybrid frameworks have partially fulfilled the expectations derived from choosing TCBA ligands together with hydroxyl groups as structure-directing agents.

Depending on the metal cations, the coordination modes of TCBA ligands as well as OH groups can have profound effects in the diverse structures of **1**−**3**. In all these three inorganic−organic hybrid framework materials, there are three crystallographically independent M(II) cations. The coordination numbers of Zn complexes are 6, 6 and 4. those of Co complex are 6, 6 and 6. OH groups exhibit two kinds of μ_3-bridging modes in **3**, they link Co^{2+} cations to hexameric clusters. In **1** and **2**, OH groups only show one kind of μ_3-bridging mode and join Zn^{2+} ions to centrosymmetric pentameric clusters.

TCBA ligands show rich coordination modes in **1**−**3** and join Zn^{2+}, or Co^{2+} cations to high dimensional metal−organic frameworks. Furthermore, TCBA ligand plays a key role for the formation of multi-stranded helix structures in the metal-organic frameworks of **1**−**3**. This is most likely due to that it owns one rigid carboxyl group and three flexible O-acetate groups with a total of eleven possible coordination sites. The function groups also branch out with multiple angles of 60º, 120º and 180º. Thus TCBA is able to link Zn^{2+} or Co^{2+} cations to different double-stranded chains in **1**−**3**.

Another interesting observation is the reaction temperature. The synthesis conditions of **1** and **2** were almost identical except the reaction temperatures. At the reaction temperature of 120 °C, **1** has been formed and it has four coordination and one lattice water molecules in its asymmetric unit. When the reaction was raised to 175 °C, fewer solvent molecules was involved in the formation of **2** that only contains one coordination water molecule and thus a different structure. **2** with fewer water molecules shows higher thermal stability than **1**, which may be a helpful inspiration for finding ways to improve thermal stability of hybrid frameworks.

PXRD and Themal analysis. In order to check the phase purity, these hybrid materials have been studied by using the powder X-ray diffraction (PXRD) at room temperature (see Fig. S1.†). The results from the bulk samples of **1**−**3** corroborate well with those simulated from the single crystal date respectively. The powder X-ray diffraction studies have confirmed that all the as-synthesized bulk samples of **1**−**3** are pure single phase hybrid materials.

Thermogravimetric analysis has been carried out to examine the thermal stabilities of the **1**−**3**. The initial weight loss in each complex comes from the loss of all water molecules including both lattice water and coordinated water molecules. The amount of water release is consistent with the compositions of **1**−**3**. The weight loss of 14.84 % in **1** over the temperature range of 50−266 °C is consistent with the calculated value of 14.74 % that is derived from expelling one lattice water molecule and four coordinated water molecules. **2** loses 3.78 % weight from 210 to 270 °C that corroborates the value of 3.34 % from losing one coordinated water molecule. The first weight loss in **3** between 70 and 260 °C is 16.67 % that matches 16.39 % loss corresponding to the release of two lattice water molecules and four coordinated water molecules (see Fig. S2.†).

Photophysical Properties. Complexes **1** and **2** exhibit a solid-state luminescent property at ultraviolet light, the emission spectra of complexes **1** and **2** and H_4TCBA ligands in the solid state at room temperature are investigated, as depicted in Fig. 7. The pure solid H_4TCBA ligands show an emission band at 341 nm upon the excitation at 280 nm, which can be considered as the n→π* electron transition.[17] **1** exhibits an emission maximum at 387 nm upon excitation at 310 nm with a red shift of 46 nm in contrast to H_4TCBA ligands; **2** exhibits an emission maximum at 337 nm upon excitation at 283 nm with a blue shift of 4 nm in contrast to H_4TCBA ligands. The resemblance between the emission spectrum of **1** and **2** and that of free ligands H_4TCBA indicates that the luminescence of **1** and **2** is due to a π*→π electronic transition of H_4TCBA ligands.[18] The fluorescent intensities of **1** and **2** are stronger than that of pure H_4TCBA ligands. The enhancement of luminescence may be attributed to high dimensional condensed structures of **1** and **2**, which effectively increases the rigidity of the ligands and reduces the loss of energy through the intra-ligand radiationless decay from emission excited state.[19] The red or blue shifts observed for the emissions of **1** and **2** compared to pure H_4TCBA ligands are most probably due to different coordination modes of H_4TCBA ligands and different metal-organic frameworks of **1** and **2**.[20]

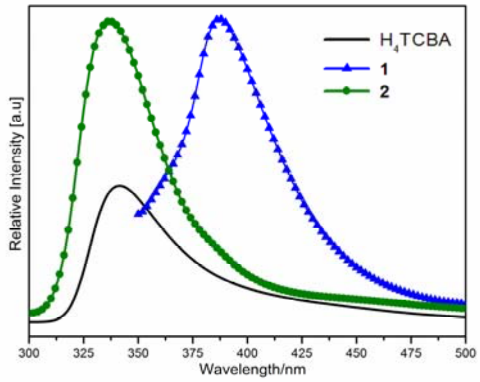

Fig. 7 Fluorescent emission spectra for H_4TCBA and **1** and **2** in the solid at room temperature.

Partial spin-crossover in complex 3. DC magnetic susceptibility study has been carried out on the bulk powder sample of hybrid complex **3** in the temperature range of 5−355 K under an applied magnetic field of 0.1 T (Fig. 8). The magnetic data shows this complex as a typical paramagnetic system and Co(II) cations can be treated as magnetically isolated from each other. The $1/\chi$ *vs* T plot clearly indicates a change in total spin as temperature decreases below 35 K (inset in Fig. 8). Data simulation using Curie's Law provides a $\chi_M T$ value of 13 cm^3K/mol between 35−355 K. This value corresponds to a total spin quantum number of 4.6 and about total 9 unpaired electrons in the three Co(II) cations per formula. Below 35 K, the $\chi_M T$ value decreases to 5 cm^3K/mol that matches with S = 2.7 and about total 5 unpaired electrons among three Co(II) cations. All Co(II) cations have the octahedral coordination in complex **3**. Although these octahedrons are slightly distorted, it is easier to understand the temperature-dependent spin change here that O_h symmetry of a perfect octahedron is used as an approximate for electron configuration of Co(II) cations in this complex. The seven valence electrons of Co(II) occupy the 3d orbitals as a high spin case of $t_{2g}^5e_g^2$ above 35 K and generate a total of 9 unpaired electrons for three Co(II) cations per formula. When the temperature decreases, two Co(II) cations change their electron configuration to the low spin $t_{2g}^6e_g^1$ case, which gives one unpaired electron for each of these two Co(II) cations. However, the third Co(II) cation still remains at a high spin state. The total unpaired electrons become 5 at low temperature for the three Co(II) cations per formula. Since these three Co(II) cations are crystallographically independent and have very diverse inner coordination spheres, such a partial spin-crossover certainly is understandable.

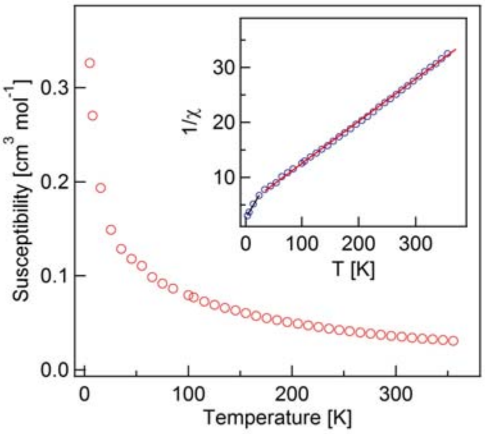

Fig. 8 Variable-temperature magnetic susceptibility plot for complex **3**.

Conclusions

In conclusion, TCBA has been used as structure-directing agent to prepare three new inorganic-organic hybrid frameworks based on polynuclear metal-hydroxyl clusters. The topology analyses show that hydroxyl groups act as effective bridges in the formation of polynuclear metal clusters and to construct highly-connected frameworks. The multiple coordination system originated from the branching out carboxylate groups in TCBA ligands results in the formation of the multi-stranded helical chains in the high-dimensional metal−organic frameworks of **1**−**3**. Complexes **1** and **2** display strong fluorescent emission at ultraviolet light. Complex **3** shows typical paramagnetic behavior and an interesting partial spin-crossover has been observed.

Notes and references

[a] *School of Environment and Chemical Engineering, Nanchang Hangkong University, Nanchang, Jiangxi, 330063, China. Fax: +86-791/86453231; Tel: +86-791/86453231; E-mail: cbliu2002@163.com*
[b] *State Key Laboratory of Food Science and Technology, Nanchang University, Nanchang, Jiangxi, 330047, China*
[c] *School of Chemistry and Biochemistry, Georgia Institute of Technology, Atlanta, Georgia 30332, United States*
[d] *School of Chemistry and Biochemistry, The Ohio State University-Columbus, Columbus, Ohio 43210, United States*

† Electronic Supplementary Information (ESI) available: X-ray crystallographic files in CIF format for **1**−**3**, selected bond lengths and angles, and the selected hydrogen bonding lengths and angles of complexes **1**−**3**, PXRD pattern of **1**−**3**, TGA curves of **1**−**3**. For ESI and crystallographic data in CIF or other electronic format. See DOI: 10.1039/b000000x/

Conflict of interest

The authors declare no competing financial interest.

Acknowledgements

This work was supported by the National Natural Science Foundation of China (Nos. 21264011 and 20961007), the Aviation Fund (No. 2014ZF56020) and the Young Scientists Program of Jiangxi Province (No. 2008DQ00600) and the Voyage Project of Jiangxi Province.

1 (a) R. B. Getman, Y. S. Bae, C. E. Wilmer and R. Q. Snurr, *Chem. Rev.*, 2012, **112**, 703; (b) J. R. Li, J. Sculley and H. C. Zhou, *Chem. Rev.*, 2012, **112**, 869; (c) Y. N. Gong, Y. L. Huang, L. Jiang and T. B. Lu, *Inorg. Chem.*, 2014, **53**, 9457.
2 (a) K. K. Bania, G. V. Karunakar, K. Goutham and R. C. Deka, *Inorg. Chem.*, 2013, **52**, 8017; (b) R. Ramnauth, S. Al-Juaid, M. Motevalli, B. C. Parkin and A. C. Sullivan, *Inorg. Chem.*, 2004, **43**, 4072.
3 (a) Y. J. Cui, Y. F. Yue, G. D. Qian and B. L. Chen, *Chem. Rev.*, 2012, **112**, 1126; (b) L. M. Fan, W. L. Fan, B. Li, X. Z. Liu, X. Zhao and X. T. Zhang, *RSC Adv.*, 2015, **5**, 14897; (c) B. M. Ji, D. S. Deng, J. Y. Ma, C. W Sun and B. Zhao, *RSC Adv.*, 2015, **5**, 2239; (d) Y. E. Cha, X. Li, D. Ma and R. Huo, *Eur. J. Inorg. Chem.*, 2014, 2969; (e) A. Hens and K. K. Rajak, *RSC Adv.*, 2015, **5**, 4219.
4 (a) W. B. Chen, Z. X. Li, Z. J. Ouyang, W. N. Lin, L. Yang and W. Dong, *RSC Adv.*, 2014, **4**, 61104; (b) J. Z. Qiao, M. S. Zhan and T. P. Hu, *RSC Adv.*, 2014, **4**, 62285; (c) M. J. Murphy, P. M. Usov, F. J. Rizzuto, C. J. Kepert and D. M. D′Alessandro, *New J. Chem.*, 2014, **38**, 5856; (d) G. S. Yang, C. B. Liu, H. Liu, J. Robbins, Z. J. Zhang, H. S. Yin, H. L. Wen and Y. H. Wang, *J. Solid State Chem.*, 2015, **225**, 391; (e) J. P. Zhao, R. Zhao, W. C. Song, Q. Yang, F. C. Liu and X. H. Bu, *Cryst. Growth Des.*, 2013, **13**, 437.
5 (a) G. S. Yang, C. B. Liu, H. L. Wen, S. S. Tan and Z. J. Zhang, *CrystEngComm*, 2015, **17**, 1518; (b) K. Z. Shao, Y. H. Zhao, Y. Q. Lan, X. L. Wang, Z. M. Su and R. S. Wang, *CrystEngComm*, 2011, **13**, 889; (c) Y. X. Ren, S. S. Xiao, X. J. Zheng, L. C. Li and L. P. Jin, *Dalton Trans.*, 2012, **41**, 2639; (d) A. Patra, T. K. Sen, R. Bhattacharyya, S. K. Mandal and M. Bera, *RSC Adv.*, 2012, **2**, 1774; (e) J. Tao, J. X. Shi, M. L. Tong, X. X. Zhang and X. M. Chen, *Inorg. Chem.*, 2001, **40**, 6328.
6 (a) B. Moulton and M. J. Zaworotko, *Chem. Rev.*, 2001, **101**, 1629; (b) M. Xue, G. S. Zhu, H. Ding, L. Wu, X. J. Zhao, Z. Jin and S. L. Qiu, *Cryst. Growth Des.*, 2009, **9**, 1481; (c) K. Biradha, M. Sarkar and L. Rajput, *Chem. Commun.*, 2006, 4169.
7 (a) X. Liu and K. L. Huang, *Inorg. Chem.*, 2009, **48**, 8653; (b) X. S. Qu, L. Xu, G. G. Gao, F. Y. Li and Y. Y. Yang, *Inorg. Chem.*, 2007, **46**, 4775; (c) Q. Chen, J. B. Lin, W. Xue, M. H. Zeng and X. M. Chen, *Inorg. Chem.*, 2011, **50**, 2321; (d) D. S. Li, J. Zhao, Y. P. Wu, B. Liu, L. Bai, K. Zou and M. Du, *Inorg. Chem.*, 2013, **52**, 8091; (e) A. J. Cairns, J. A. Perman, L. Wojtas, V. C. Kravtsov, M. H. Alkordi, M. Eddaoudi and M. J. Zaworotko, *J. Am. Chem. Soc.*, 2008, **130**, 1560.
8 A. K. Cheetham, C. N. R. Rao and R. K. Feller, *Chem. Commun.*, 2006, 4780.
9 (a) L. F. Ma, L. Y. Wang, M. Du and S. R. Batten, *Inorg. Chem.*, 2010, **49**, 365; (b) X. P. Li, J. Y. Zhang, M. Pan, S. R. Zheng, Y. Liu and C. Y. Su, *Inorg. Chem.*, 2007, **46**, 4617; (c) Q. Gao, F. L. Jiang, M. Y. Wu, Y. G. Huang, W. Wei and M. C. Hong, *Cryst. Growth Des.*, 2010, **10**, 184; (d) M. Ikeda, Y. Tanaka, T. Hasegawa, Y. Furusho and E. Yashima, *J. Am. Chem. Soc.*, 2006, **128**, 6806; (e) K. Dhara, J. Ratha, M. Manassero, X. Y. Wang, S. Gao and P. Banerjee, *J. Inorg. Biochem.*, 2007, **101**, 95; (f) I. G. Filippova, O. A. Gherco, Y. A. Simonov, A. A. Deseatnic-Ciloci, S. F. Clapco, J. P. Tiurina, S. G. Baca, *Polyhedron*, 2010, **29**, 1102; (g) Q. B. Bo, H. T. Zhang, J. L. Miao and Z. W. Zhang, *Eur. J. Inorg. Chem.*, 2013, 5631.
10 L. Han and M. C. Hong, *Inorg. Chem. Commun.*, 2005, **8**, 406.
11 (a) T. J. Prior and M. J. Rosseinsky, *Inorg. Chem.*, 2003, **42**, 1564; (b) N. Guillou, C. Livage, M. Drillon and G. Férey, *Angew. Chem., Int. Ed.*, 2003, **42**, 5314.
12 (a) C. J. Kepert, T. J. Prior and M. J. Rosseinsky, *J. Am. Chem. Soc.*, 2000, **122**, 5158; (b) X. Li, R. Cao, Y. Q. Sun, Q. Shi, D. Q. Yuan, D. F. Sun, W. H. Bi and M. C. Hong, *Cryst. Growth Des.*, 2004, **4**,

255; (c) L. Han, M. C. Hong, R. H. Wang, J. H. Luo, Z. Z. Lin and D. Q. Yuan, *Chem. Commun*., 2003, 2580; (d) R. H. Wang, Y. F. Zhou, Y. Q. Sun, D. Q. Yuan, L. Han, B. Y. Lou, B. L. Wu and M. C. Hong, *Cryst. Growth Des*., 2005, **5**, 251; (e) Y. F. Zhou, F. L. Jiang, Y. Xu, R. Cao and M. C. Hong, *J. Mol. Struct*., 2004, **691**, 191; (f) Y. Xu, L. Han, Z. Z. Lin, C. P. Liu, D. Q. Yuan, Y. F. Zhou and M. C. Hong, *Eur. J. Inorg. Chem*., 2004, 4457; (g) S. S. Massoud, F. A. Mautner, F. R. Louka, S. Demeshko, S. Dechert and F. Meyer, *Inorg. Chim. Acta*., 2011, **370**, 435; (h) F. A. Mautner, J. H. Albering, R. Vicente, C. Andrepont, J. G. Gautreaux, A. A. Gallo and S. S. Massoud, *Polyhedron*, 2013, **54**, 158.

13 Y. H. He, Y. L. Feng, Y. Z. Lan and Y. H. Wen, *Cryst. Growth Des*., 2008, **8**, 3586.

14 G. M. Sheldrick, *SADABS*, *Program for Empirical Absorption Correction of the Area detector Data*, University of Göttingen, Germany, 1997.

15 G. M. Sheldrick, *SHELXS 97*, *Program for Crystal Structure Solution*, University of Göttingen, Germany, 1997.

16 G. M. Sheldrick, *SHELXL 97*, *Program for Crystal Structure Refinement*, University of Göttingen, Germany, 1997.

17 P. F. Shi, Z. Chen, G. Xiong, B. Shen, J. Z. Sun, P. Cheng and B. Zhao, *Cryst. Growth Des*., 2012, **12**, 5203.

18 (a) Z. F. Tian, J. G. Lin, Y. Su, L. L. Wen, Y. M. Liu, H. Z. Zhu and Q. J. Meng, *Cryst. Growth Des*., 2007, **7**, 1863; (b) Y. N. Chi, K. L. Huang, S. W. Zhang, F. Y. Cui, Y. Q. Xu and C. W. Hu, *Cryst. Growth Des*., 2007, **7**, 2449.

19 (a) Y. N. Gong, C. B. Liu, H. L. Wen, L. S. Yan, Z. Q. Xiong and L. Ding, *New J. Chem*., 2011, **35**, 865; (b) X. L. Yang, M. H. Xie, C. Zou and C. D. Wu, *CrystEngComm*, 2011, **13**, 6422.

20 P. C. Cheng, P. T. Kuo, Y. H. Liao, M. Y. Xie, W. Hsu and J. D. Chen, *Cryst. Growth Des*., 2013, **13**, 623.

TOC graphic for

Self-assembly, crystal structures and properties of metal-3,4,5-tris (carboxymethoxy)benzoic acid frameworks based on polynuclear metal-hydroxyl clusters (M = Zn, Co)

Gaoshan Yang,[a] Huiliang Wen,[b] Chongbo Liu,[*ac] Julianne Robbins,[c] Yunhan Wen[d] and Z. John Zhang[*c]

Three new inorganic-organic frameworks based on 3,4,5-tris(carboxymethoxy)benzoic acid and polynuclear metal-hydroxyl clusters were assembled. Photoluminescent and magnetic properties are investigated.